Journal of Histochemistry & Cytochemistry 59(2) 188–201

DOI: 10.1369/0022155410394859
http://jhc.sagepub.com
SAGE

Expression of C4.4A, a Structural uPAR Homolog, Reflects Squamous Epithelial Differentiation in the Adult Mouse and during Embryogenesis

Mette C. Kriegbaum, Benedikte Jacobsen, Andreas Hald, and Michael Ploug
The Finsen Laboratory, Rigshospitalet Section 3735, Copenhagen, Denmark (MCK,BJ,MP); Institute for Cellular and Molecular Medicine, University of Copenhagen, Copenhagen, Denmark (AH); and Danish-Chinese Centre for Proteases and Cancer (MP)

Summary

The glycosylphosphatidylinositol (GPI)–anchored C4.4A was originally identified as a metastasis-associated protein by differential screening of rat pancreatic carcinoma cell lines. C4.4A is accordingly expressed in various human carcinoma lesions. Although C4.4A is a structural homolog of the urokinase receptor (uPAR), which is implicated in cancer invasion and metastasis, no function has so far been assigned to C4.4A. To assist future studies on its function in both physiological and pathophysiological conditions, the present study provide a global survey on C4.4A expression in the normal mouse by a comprehensive immunohistochemical mapping. This task was accomplished by staining paraffin-embedded tissues with a specific rabbit polyclonal anti-C4.4A antibody. In the adult mouse, C4.4A was predominantly expressed in the suprabasal layers of the squamous epithelia of the oral cavity, esophagus, non-glandular portion of the rodent stomach, anus, vagina, cornea, and skin. This epithelial confinement was particularly evident from the abrupt termination of C4.4A expression at the squamo-columnar transition zones found at the ano-rectal and utero-vaginal junctions, for example. During mouse embryogenesis, C4.4A expression first appears in the developing squamous epithelium at embryonic day 13.5. This anatomical location of C4.4A is thus concordant with a possible functional role in early differentiation of stratified squamous epithelia. (J Histochem Cytochem 59:188–201, 2011)

Keywords

LYPD3, squamous epithelium differentiation, squamo-columnar junctions, uPAR, biomarker, NSCLC, stratum spinosum, immunohistochemistry, mouse

A massive research effort is currently being devoted to identifying and characterizing new biomarkers with expression profiles providing diagnostic and prognostic information on cancer progression and dissemination (Ullah and Aatif 2009). Ultimately, such information may guide individualized patient management, including the selection of optimal intervention regimens and subsequent monitoring of treatment efficacy. One such potential tumor biomarker is C4.4A, which was first identified in an unbiased immunological screen designed to select membrane proteins that were differentially expressed by highly metastasizing rat pancreatic cell lines (Claas et al. 1996). On the basis of this selection criterion, Zöller and coworkers classified C4.4A as a metastasis-associated protein (Claas et al. 1996). Several independent studies have subsequently investigated the expression pattern of C4.4A in various human malignancies with particular emphasis on human carcinoma lesions and their corresponding

Supplementary material for this article is available on the *Journal of Histochemistry & Cytochemistry* Web site at http://jhc.sagepub.com/supplemental.

Received for publication October 6, 2010; accepted November 23, 2010

Corresponding Author:
Michael Ploug, Finsen Laboratory, Rigshospitalet Section 3537, Copenhagen Biocenter room 3.3.31, Ole Maaløes Vej 5, DK-2200 Copenhagen N, Denmark.
E-mail: m-ploug@finsenlab.dk

metastases. In two small pilot studies by in situ hybridization, expression of C4.4A mRNA was observed in melanomas (Seiter et al. 2001) and in urothelial transitional cell carcinomas (Smith et al. 2001). In both cases, lymph node metastases were also C4.4A positive. Along the same lines of evidence, an immunohistochemical study demonstrated that the C4.4A protein is expressed at the invasive front of esophageal squamous cell carcinoma as well as in the corresponding lymph node metastases (Hansen et al. 2008). Particularly intriguing is, however, the recent observation that although normal lung tissue is devoid of C4.4A as probed by Northern blotting, RT-PCR, or immunohistochemistry (Claas et al. 1996; Würfel et al. 2001), high expression of C4.4A is nonetheless a strong and independent prognostic biomarker for poor survival in patients with non–small cell lung cancer (NSCLC; Hansen et al. 2007). This relationship pertains in particular to the histological subgroup of lung cancer patients having adenocarcinoma lesions. Although these data clearly highlight C4.4A as a promising biomarker for poor prognosis in this group of lung cancer patients, a causal relationship responsible for this correlation is not evident, given that a well-defined biochemical function has so far not been assigned to C4.4A. Nevertheless, circumstantial evidence has prompted the speculations that C4.4A may be involved in either cell-matrix interactions (Paret et al. 2005; Rösel et al. 1998; Smith et al. 2001) or in cell-cell adhesion (Hansen et al. 2008).

The gene for human C4.4A (*LYPD3*) is located in a small cluster on chromosome 19q13 along with four other genes encoding homologous proteins, including the gene for the urokinase-type plasminogen activator receptor (uPAR), *PLAUR* (Jacobsen and Ploug 2008; Kjaergaard et al. 2008). These proteins are all glycosylphosphatidylinositol (GPI)-anchored, and their extracellular domains are composed of two to three modules belonging to the Ly6/uPAR/α-neurotoxin (LU) protein domain family (Ploug 2003). As opposed to C4.4A, uPAR has a well-established and nonredundant biochemical function in focalizing uPA-mediated plasminogen activation to cell surfaces (Ploug 2003), and this cell-bound proteolytic activity assists extravascular fibrin surveillance (Connolly et al. 2010). Like C4.4A, high expression levels of uPAR are correlated with poor patient survival in a number of human cancers (Høyer-Hansen and Lund 2007). An important distinction is, however, that whereas uPAR predominantly is expressed by tumor-reactive stromal cells, C4.4A is expressed by the carcinoma cells. The crystal structures solved for human and mouse uPAR reveal that this protein is composed of three LU modules forming a large hydrophobic ligand-binding cavity (Huai et al. 2006; Lin et al. 2010). From bioinformatic considerations, it is evident that C4.4A is composed of two N-terminal LU modules, which are joined to the glycolipid anchor by a C-terminal linker region modified with O-linked carbohydrate (Hansen et al. 2004). Homology considerations reveal that the two N-terminal LU domains of C4.4A exhibit a much larger degree of sequence conservation between man and mouse than that observed between the corresponding uPAR orthologs (89% vs 60%; see Suppl. Fig. S1), and this evolutionary conservation may actually signify that C4.4A serves an important physiological function. From a more practical point of view, this evolutionary conservation of C4.4A explains why our rabbit polyclonal antibody raised against purified human C4.4A (Hansen et al. 2004) can be used to detect the orthologous mouse and rat protein, which is exploited in the current immunohistochemical study.

To obtain a more complete description of the global expression profiles of C4.4A during normal physiology, we embarked in the present study on mapping its expression in the adult mouse as well as during embryogenesis. This information is important for future studies on the impact of C4.4A on cancer progression in the numerous mouse models that are presently used as surrogates for the corresponding human diseases (Bos et al. 2010). This expression roadmap for C4.4A also represents an important guideline for dissection of any overt or induced phenotypic changes in mice with a disrupted *Lypd3* gene.

Materials and Methods

Animals and Tissues

FVB/N mice (12 weeks old) and Sprague Dawley rats (8 weeks old) were anesthetized using 0.1 ml/10 g of a 1:1 mixture of Hypnorm (fluanison 5 mg/ml and fentanyl 0.1 mg/ml) and Dormicum (midazolam 5 mg/ml) before they were perfused with PBS followed by 4% (v/v) buffered formalin. Embryos from FVB/N mice were generated by time-controlled mating with estimation of the ages from the appearance of a vaginal plug (E0.5). Embryos of day E9.5 and days E13.5 to E18.5 were collected from the euthanized pregnant mice. Newborn pups were also included. Dissected organs, embryos, and newborn mice were formalin fixed overnight prior to paraffin embedment. Mouse esophagi were collected from euthanized animals for protein extraction and subsequently frozen at –20C until use. Mice were housed in a certified facility, and the study was carried out in accordance with institutional guidelines.

Antibodies and Proteins

Rabbit polyclonal antibody against human C4.4A was produced and purified in house as previously described (Hansen et al. 2004). Rabbit immunoglobulin of irrelevant specificity (code no. x0903) and horseradish peroxidase–conjugated swine anti-rabbit antibody (code no. P0217) were purchased from Dako (Glostrup, Denmark). Horseradish peroxidase–labeled EnVision rabbit reagent (code no. K4003) was from Dako (Carpenteria, CA). Recombinant human C4.4A fused

to the third domain of uPAR (C4.4A-uPAR DIII) was produced and purified as described (Gårdsvoll et al. 2007; Hansen et al. 2004).

Detection of C4.4A in Tissue Extracts by Western Blotting

Mouse esophagi were snap-frozen in liquid nitrogen prior to mechanical homogenization. Protein extraction was subsequently performed by addition of 5 µl extraction buffer (0.1 M Tris [pH 7.4], 1% [v/v] Triton X-114, including 1:25 [v/v] Complete Proteinase Inhibitor Cocktail from Roche [Mannheim, Germany]) per mg of tissue. The suspension was mixed thoroughly and left on ice for 25 min prior to three bursts of ultrasonication of 7 min each. Finally, the lysate was clarified by centrifugation at 4C, 12,000 × g for 30 min, and the supernatant was subjected to temperature-induced detergent phase separation at 37C for 5 min. The detergent phase containing the GPI-anchored C4.4A was collected at 37C by centrifugation for 15 min at 12,000 × g and subjected to SDS-PAGE separation (NuPAGE system; Invitrogen, Carlsbad, CA). Proteins were subsequently immobilized on a polyvinylidene difluoride (PVDF) membrane (Millipore; Bedford, MA) by electrophoretic transfer using a Bio-Rad Criterion Blotter (Hercules, CA) with a solution of 12 mM Tris, 96 mM glycine (pH 8.3), and 20% (v/v) ethanol as transfer buffer. Excess protein binding sites were blocked in 2% (w/v) BSA, and the PVDF membrane was incubated with 0.1 µg/ml of rabbit polyclonal anti-C4.4A antibody overnight at 4C. The bound polyclonal antibody was detected with horseradish peroxidase–conjugated swine anti-rabbit antibody (1:25,000 [v/v]), and the reaction was visualized with enhanced chemiluminescence using the ECL detection reagent from Amersham Biosciences (Burlinghamshire, UK). Control of specificity included a 1-hr preincubation of the polyclonal rabbit anti-C4.4A antibody with a 10-fold molar excess of purified recombinant C4.4A-uPAR DIII prior to probing.

Immunohistochemical Detection of C4.4A

Paraffin-embedded tissue sections (5 µm) were mounted on superfrost plus glass slides (Thermo Scientific; Braunschweig, Germany), deparaffinized in xylene, and hydrated through a series of ethanol/water solutions. Antigen retrieval was achieved by pretreatment with 5 µg/ml proteinase K for 10 min at 37C. Endogenous peroxidase activity was blocked by incubation in 1% (v/v) H_2O_2 for 15 min. The sections were washed in Tris-buffered saline (50 mM Tris, 150 mM NaCl, pH 7.6) containing 0.5% (v/v) Triton X-100 before overnight incubation in Shandon racks (Thermo Shandon; Pittsburg, PA) at 4C with the primary antibody diluted in Antibody Diluent (Dako; Glostrup, Denmark) to either 2.5 µg/ml or 1 µg/ml for mouse and rat tissues, respectively. Incubation of the polyclonal anti-C4.4A antibody with a 10-fold molar excess of purified recombinant C4.4A-uPAR DIII for 1 hr prior to its addition to the tissue sections served as a rigorous specificity control. EnVision rabbit reagent was used as secondary antibody, and the sections were developed with NovaRed (Vector Laboratories; Burlingame, CA) for 9 min as specified by the manufacturer. Finally, sections were counterstained with Mayer's hematoxylin for 30 sec, dehydrated in ethanol baths, and mounted with pertex.

Results

Specificity of the Immunohistochemical Detection of C4.4A in Mouse Tissues

In the present study, the global expression profile of murine C4.4A was analyzed by immunohistochemistry using our well-characterized anti-C4.4A polyclonal antibody raised against human recombinant C4.4A (Hansen et al. 2004) on formalin-fixed and paraffin-embedded tissues. We relied on the specific cross-reactivity of this antibody with murine C4.4A, which is probably a consequence of the high degree of sequence conservation (89%) between mouse and human C4.4A, as documented in Supplementary Figure S1. To validate its use for staining of paraffin-embedded mouse tissue, we initially performed a number of control experiments. First, adjacent sections from an adult FVB/N mouse esophagus were selected as positive control tissue because of the pronounced C4.4A expression we had observed previously in the suprabasal layer of the stratified squamous epithelium of human esophagus (Hansen et al. 2008). Reassuringly, we recapitulated a prominent staining of the squamous epithelium of mouse esophagus using this polyclonal anti-C4.4A antibody raised against the human ortholog. Importantly, this immunohistochemical staining exhibited a distinct membrane-bound morphology restricted to stratum spinosum and leaving the basal layer as well as stratum granulosum negative (Fig. 1A,B), thus recapitulating the expression pattern published for the human esophagus (Hansen et al. 2008). Second, the specificity of this staining was further validated, as it could be completely abrogated by a preincubation of the polyclonal antibody with recombinant C4.4A-uPAR DIII (Fig. 1C,D). Third, IgG with an irrelevant specificity purified from a non-immunized rabbit showed no specific reaction with the epithelium when applied at the same concentration (Fig. 1E). As a last quality control on the specificity of the cross-reactivity with murine C4.4A, we subjected detergent phase extracts from mouse esophagus to Western blotting using the reactivity of our polyclonal anti-C4.4A antibody for detection of murine C4.4A in this complex protein mixture. As shown in Figure 1F (lane 3), only one component was

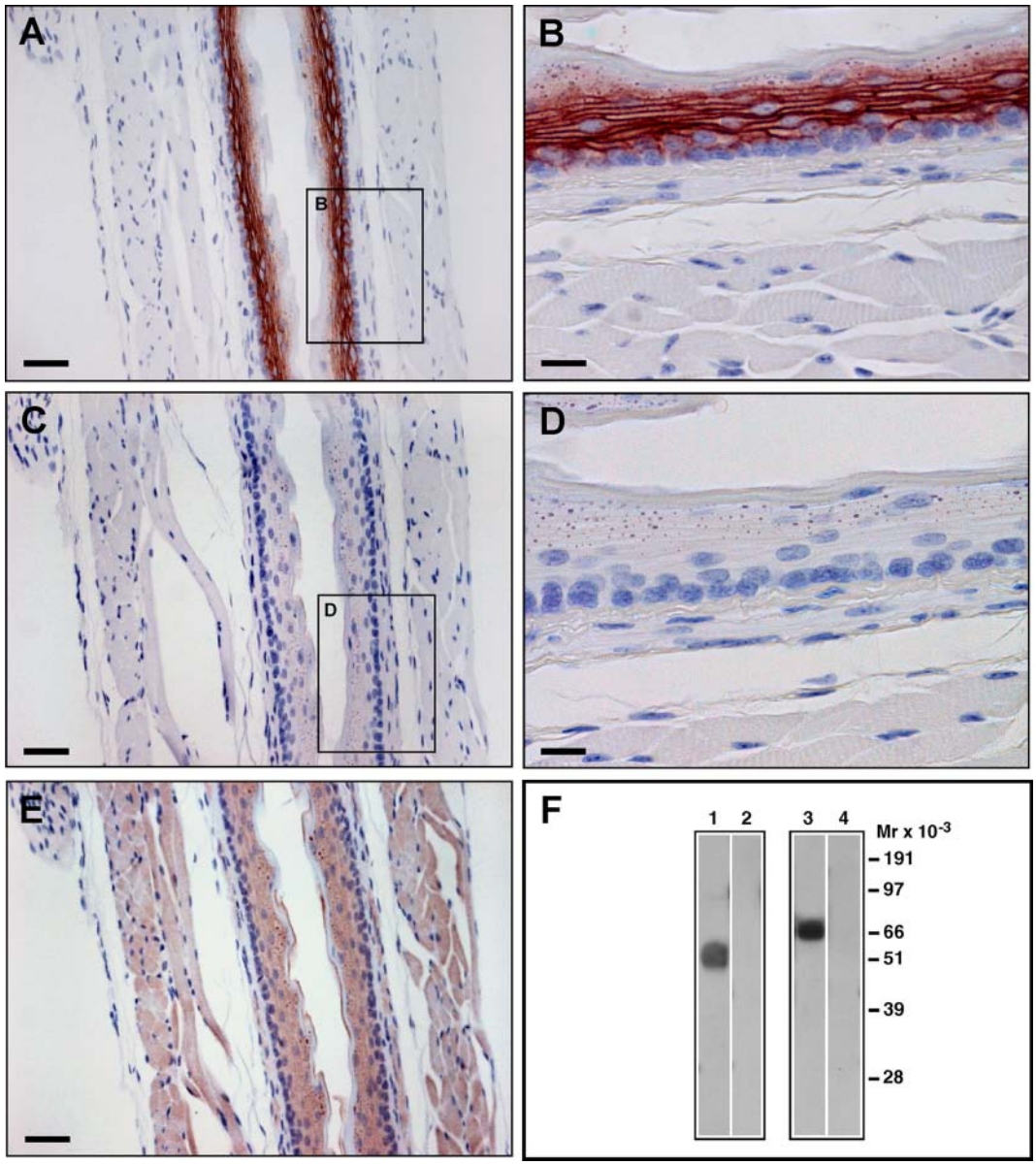

Figure 1. Specificity of the cross-reaction of polyclonal rabbit anti-human C4.4A antibody with murine C4.4A. Immunohistochemistry was performed on serial sections of adult murine esophagus incubated with 2.5 µg/ml polyclonal anti-C4.4A antibody alone (A, B) or after preincubation with a 10-fold molar excess of purified recombinant human C4.4A-uPAR DIII (C, D). A higher magnification of the squamous epithelium (B) reveals a pronounced membrane-associated C4.4A staining, which is eliminated after antibody preabsorption (D). A negative control IgG with irrelevant specificity (2.5 µg/ml) did not stain the squamous epithelium at all (E). Panel F shows immunoblots of 0.02 µg recombinant human C4.4A-uPAR DIII (positive control; lanes 1 and 2) and detergent phase extracts from murine esophagus (lanes 3 and 4) incubated with polyclonal anti-C4.4A antibody either alone (lanes 1 and 3) or after preincubation with a 10-fold molar excess of purified recombinant human C4.4A-uPAR DIII (lanes 2 and 4). Scale bars = 50 µm (A, C, E) and 15 µm (B, D).

recognized by the polyclonal anti-C4.4A antibody, and this possessed the expected electrophoretic mobility of C4.4A. Note that C4.4A from natural sources has a much slower electrophoretic mobility as compared to recombinant C4.4A expressed in *Drosophila* S2 cells because of extensive differences in the N- and O-linked glycosylation (compare lanes 1 and 3; Hansen et al. 2004). Similar to the immunohistochemical detection of murine C4.4A described above, the reactivity in Western blotting could be completely abolished when preincubating with the recombinant human C4.4A-uPAR DIII (Fig. 1F, lane 4). These control experiments clearly validate the specificity of the C4.4A detection

Table 1. C4.4A Protein Expression in the Adult Mouse and Rat

Tissue	C4.4A Expression in the Adult Mouse	C4.4A Expression in the Adult Rat
Oral cavity/tongue	+[1]	+[1]
Esophagus	+[1]	+[1]
Stomach		
Glandular	–	–
Non-glandular	+[1]	+[1]
Duodenum	–	–
Jejunum	–	–
Ileum	–	–
Colon ascendes	–	–
Colon sigmoideum	–	–
Rectum	–	–
Anus	+[1]	ND
Ovaries	–	–
Uterus	–	–
Vagina	+[1]	+[1]
Testicle	–	–
Epididymis	–	–
Prostate	–	–
Seminal vesicle	–	ND
Skin	+[1]	+[1]
Hair follicle	+[1]	+[1]
Bone	–	ND
Bone marrow	–	ND
Eye		
Cornea	+[1]	+[1]
Retina	+[2]	+[2]
Adipose tissue	–	–
Brain	–	ND
Thymus	+[3]	+[3]
Spleen	–	–
Lymph node	–	–
Liver	–	–
Pancreas	–	–
Mammae	–	–
Kidney	–	–
Bladder	–	–
Heart	–	–
Striated muscle	–	–
Smooth muscle	–	–
Nasal cavity	+[1]	ND
Trachea	–	–
Lung	–	–

Abbreviations: +[1], C4.4A staining in the stratified squamous epithelium; +[2], C4.4A staining in the pigmented epithelium of the retina; +[3], C4.4A staining in Hassall's corpuscle of the thymus; –, no C4.4A staining; ND, not determined.

of the murine ortholog, thus justifying the application of this procedure to a general detection of murine C4.4A in different anatomical locations.

Histological Localization of C4.4A in the Adult Mouse

Having established the specificity of the polyclonal anti-C4.4A antibody, we continued to map the histological localization of C4.4A under physiological conditions in the mouse. A library of paraffin-embedded tissues from FVB/N mice was therefore probed for C4.4A expression using the protocol established for the staining of esophagus. All organs were examined in duplicates from two different mice, and they showed similar results in all cases. The specificity of these stainings was confirmed by preabsorption controls using the recombinant human C4.4A-uPAR DIII. The results are summarized in Table 1.

Gastrointestinal tract. An evaluation of the gastrointestinal tract revealed that C4.4A was confined to stratified squamous epithelium of the cranial end (i.e., the oral cavity, here exemplified by the tongue) and the entire length of the esophagus (Fig. 2A,B), as well as the more caudally located non-glandular part of the stomach (Fig. 2C,D). The rodent stomach is divided into two portions, the non-glandular (fundus) and the glandular (antrum) part. The esophagus of rodents terminates in the non-glandular part of the stomach, which represents a food storage compartment composed of stratified squamous epithelium (Fukamachi et al. 1979). The traditional squamo-columnar junction located at the gastroesophageal connection in humans is consequently translocated to the border between the fundus and antrum in mice, where the latter glandular portion is lined by a digestive enzyme-secreting columnar epithelium. A squamous protrusion of the lamina propria is the visible demarcation of the two areas (Fig. 2C) and the equivalent of the human gastroesophageal junction. C4.4A expression was absent in the glandular epithelium, and it appeared to follow the location of stratified squamous epithelium (Fig. 2C,D). The entire ensemble of columnar epithelia of the intestines was devoid of C4.4A expression, as exemplified by sections of duodenum and the sigmoid colon (Fig. 2E,F). At the caudal part of the gastrointestinal tract, C4.4A expression reappeared at the ano-rectal junction at the transition zone between the columnar epithelium and stratified squamous epithelium (Fig. 2G,H).

Reproductive system. C4.4A was also confined to the squamous epithelium of the reproductive system of the female mouse (i.e., the vagina; Fig. 3A,C). Paralleling the results from the gastrointestinal tract, the pronounced C4.4A expression present in the epithelium of the vagina terminated with the transition to the columnar epithelium of the uterus (Fig. 3A). This observation was, however, in contradiction to a previous report on C4.4A expression in rat tissue (Claas et al. 1996). That particular study stated that C4.4A was confined to the glandular epithelium of the uterus and also the ductal epithelium of the epididymis in the reproductive systems of the female and male rat, respectively

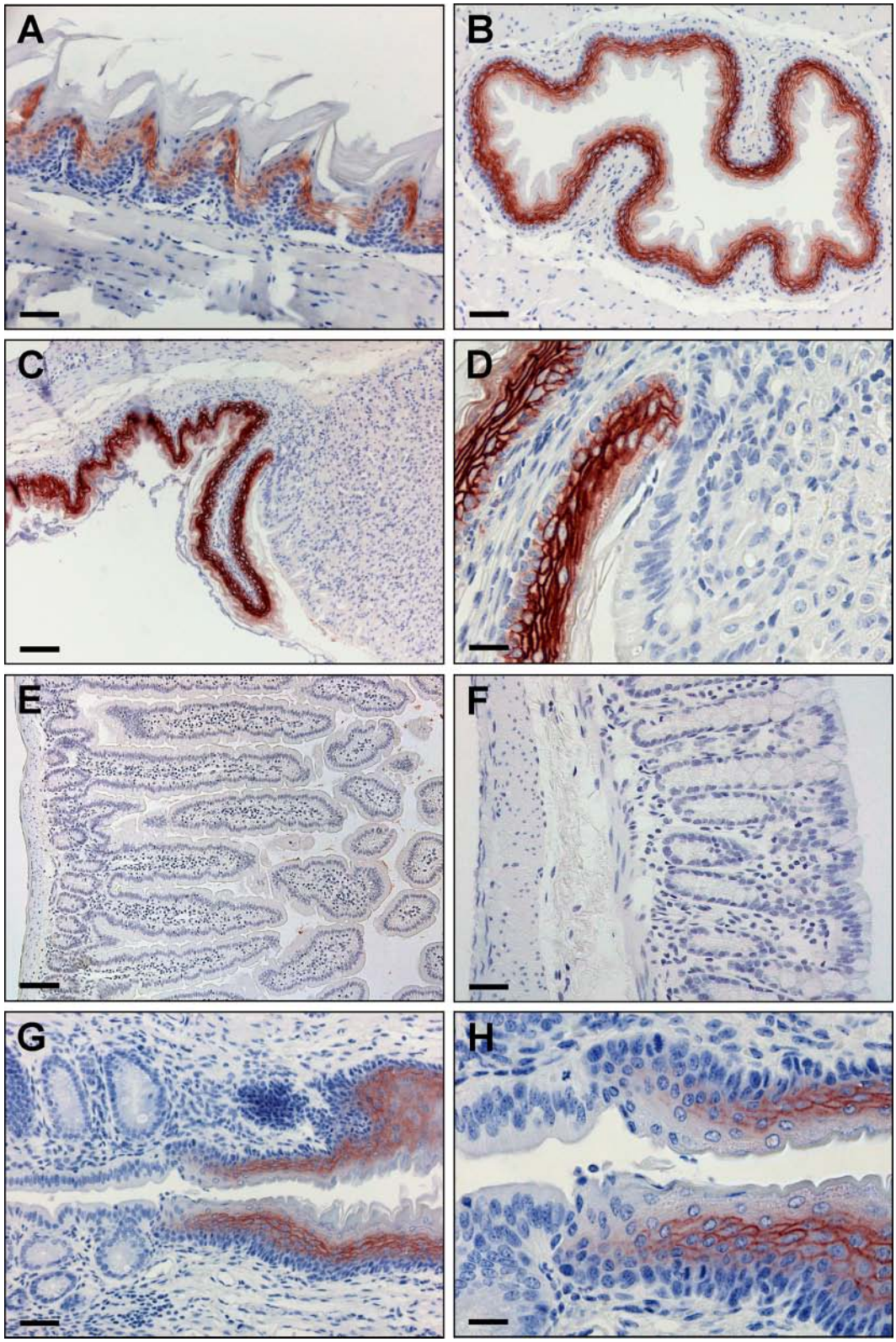

Figure 2. C4.4A expression profile in the gastrointestinal tract of the adult mouse. Sections of paraffin-embedded mouse tissue from the gastrointestinal tract were incubated with 2.5 µg/ml polyclonal anti-C4.4A antibody, the binding of which was subsequently visualized by the NovaRed chromogene. Tissues shown are tongue (A), esophagus (B), the transition zone of the non-glandular and glandular stomach regions (C, D), duodenum (E), sigmoid colon (F), and ano-rectal junction (G, H). Scale bars = 100 µm (C), 75 µm (E), 50 µm (A, B, F, G), and 25 µm (D, H).

(Claas et al. 1996). Neither of these observations, however, could be confirmed in the present study using paraffin-embedded mouse tissue (Fig. 3A,C,E).

To enable a more rigorous investigation of these apparent discrepancies, we tested whether the promiscuity of our polyclonal C4.4A antibody would allow a specific detection of rat C4.4A in formalin-fixed tissue along the same lines as we used previously for murine C4.4A (Suppl. Fig. S2). The polyclonal anti-C4.4A antibody did indeed detect rat C4.4A with high specificity, revealing the same distinct membrane-associated confinement as observed for both mouse (Fig. 1A,B) and human (Hansen et al. 2008). Successful additional specificity tests completed the validation of the antibody for immunohistochemical detection of rat C4.4A.

Mouse and rat uteri and epididymides were subsequently stained in parallel to scrutinize whether the dissimilar expression patterns reported for C4.4A in these tissues could be related to an unexpected species difference. Comparing the present immunohistochemical stainings, it is evident that no divergence in the C4.4A expression can be seen in these two rodents. C4.4A is concordantly expressed in the stratified squamous epithelia of the vagina in both mouse (Fig. 3A,C) and rat (Fig. 3B,D), whereas it is absent from the columnar epithelium of the uterus (Fig. 3A,B) and the ductal epithelium of the epididymis (Fig. 3E, F). The reason for this minor divergence in expression profile is unclear, but it should be emphasized that the present study was performed on paraffin-embedded tissue samples, whereas the previous study used snap-frozen tissue (Claas et al. 1996).

One noteworthy difference between the mouse and rat vagina is that the superficial cell layer of this particular rat vagina was devoid of C4.4A reactivity (Fig. 3B). This, however, may be related to the fact that this female rat was in the proestrus stage of the reproduction cycle, characterized by a superficial mucoid layer of cuboidal cells (Westwood 2008). The histological changes occurring in the vagina during the reproductive cycle do not occur uniformly along its length, and the caudal one-third of the vagina is permanently composed of keratinized stratified squamous epithelium, which accordingly is positive for C4.4A (Fig. 3C,D). However, as evident from Figure 3C,D, the most superficial keratinized cells lose the expression of C4.4A.

Hassall's corpuscle. In the thymus, C4.4A-expressing cells were detected in Hassall's corpuscle of the medulla (Fig. 3G). In humans, this structure is composed of islands of flattened cells closely resembling keratinized squamous epithelium, as revealed by its cytokeratin expression profile (Shezen et al. 1995). This flattened cell structure was particularly evident from the C4.4A staining in Hassall's corpuscle of the rat shown in Figure 3H.

Skin and hair follicles. As reported previously (Hansen et al. 2004), keratinocytes located in the epidermis of the skin and in the related hair follicles express C4.4A (Fig. 4A,B). The adult mouse skin consists of a basal layer and a thin suprabasal layer of C4.4A-expressing cells. In the hair follicles, C4.4A is located in the outer root sheath (Fig. 4B), which is a continuation of the epidermis and hence reveals the same morphology (Davidson and Hardy 1952). C4.4A expression was observed from the most distal part of the hair follicle all the way down just below the orifice of the sebaceous glands (Fig. 4B, arrowheads), where the expression terminated. The most proximal region of the hair follicle (the bulb), where the outer root sheath only consists of a one- to two-cell layer of very low differentiation (Ito 1986), is completely devoid of C4.4A expression.

Eye. The stratified squamous epithelium in the cornea of the eye also expresses C4.4A albeit without the distinct membrane location seen in the other stratified epithelia we have examined (Fig. 4C,D). Interestingly, a variation from the normal expression pattern of C4.4A was found in the cuboidal pigmented epithelium of the retina (pars pigmentosa), where a very pronounced and distinct C4.4A staining is confined to the basolateral cell membrane facing the Bruch's basement membrane (Fig. 4C,E).

Tissues devoid of C4.4A expression. In all other tissues examined, C4.4A expression was not detectable (see Table 1). With a view to human pathology, the lack of C4.4A protein expression in the normal and healthy lung and bladder (Fig. 4F,G) is particularly interesting as these organs are reported to express C4.4A after malignant transformation (Hansen et al. 2007; Smith et al. 2001).

Expression of C4.4A during Embryogenesis

To determine the stage at which C4.4A expression is induced during mouse embryogenesis, paraffin-embedded mouse embryos were tested for C4.4A expression by immunohistochemistry on serial sections throughout entire embryos. The embryonic days 9.5 and 13.5 to 18.5 as well as newborn mice were chosen for evaluation. The onset of C4.4A expression in the squamous epithelia of the nasal cavity, tongue, esophagus, non-glandular part of the stomach, anus, skin, and vibrissal follicles is summarized in Table 2.

No detectable C4.4A expression was found in the developmental stage at E9.5 (data not shown). At embryonic day 13.5, C4.4A expression was observed in the epithelium of the nasal cavity (Fig. 5A) and a few cells of the outermost cell layers of the paws and exterior surface of the abdomen. The earliest detectable C4.4A expression in fetal back skin was observed at day E14.5 (Fig. 5E), where the architecture of the skin comprises an approximately three-layered epithelium containing the approaching stratum spinosum (Hanson 1947). A diffuse and only faint membrane-bound expression of C4.4A was detected in this particular layer. Already at day

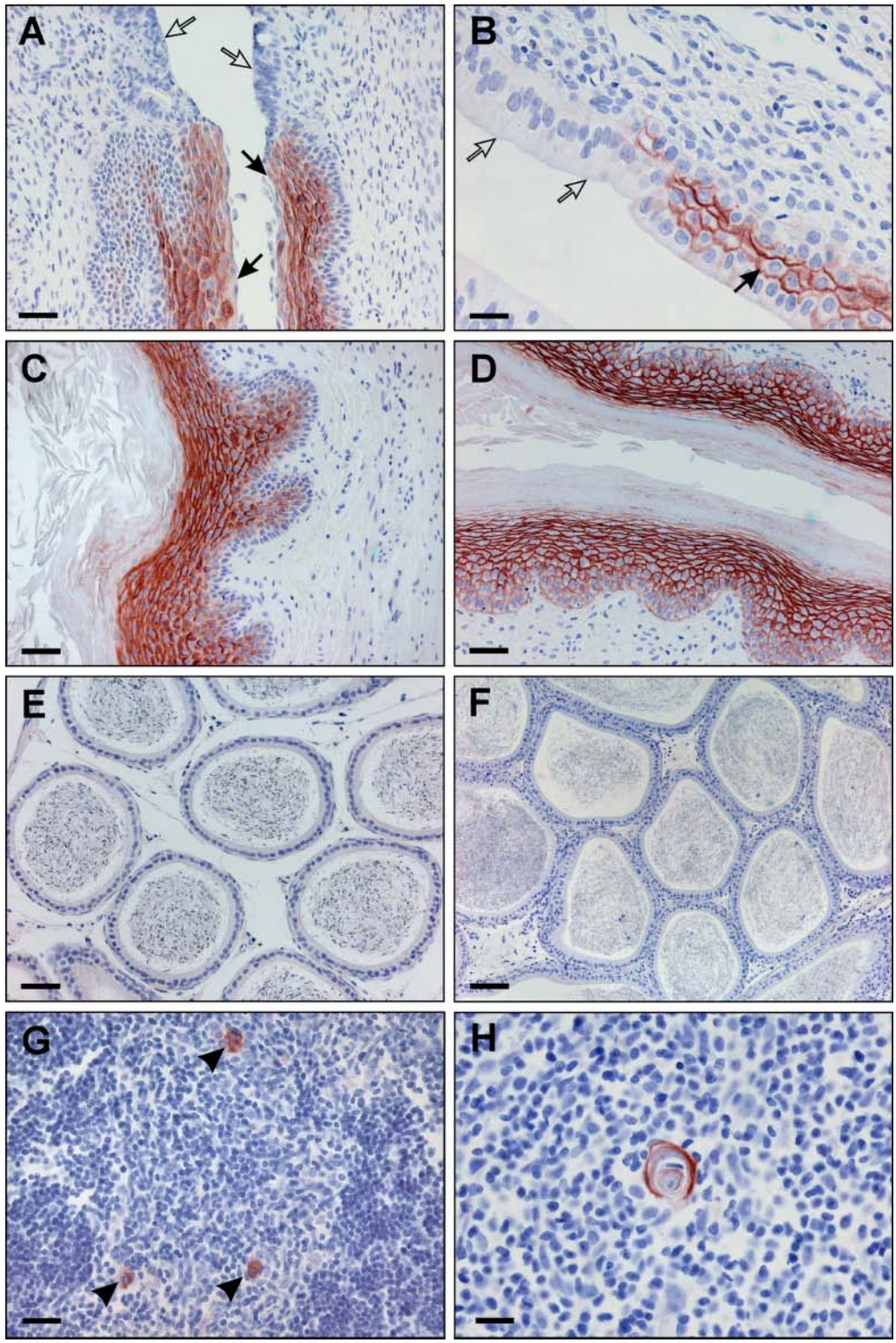

Figure 3. C4.4A expression in the mouse and rat reproductive systems and Hassall's corpuscle. The expression of C4.4A in the reproductive systems and thymus of mouse (A, C, E, G) and rat (B, D, F, H) was compared after immunohistochemical staining with the polyclonal anti-C4.4A antibody. Sections of the utero-vaginal junction (A, B), the caudal vagina (C, D), the epididymis (E, F), and thymus (G, H) were analyzed using 2.5 µg/ml or 1 µg/ml polyclonal rabbit anti-C4.4A antibody for mouse and rat tissue, respectively. In panels A and B, columnar epithelium of the uterus is indicated by open arrows, whereas squamous epithelium of the vagina is shown with black arrows. C4.4A detected in Hassall's corpuscle of the medulla of the thymus is indicated by arrowheads in panel G.A magnification of one of the squamous-like structures in the rat thymus is shown in panel H. Scale bars = 100 µm (F), 50 µm (A, C, D, E), and 25 µm (B, G, H).

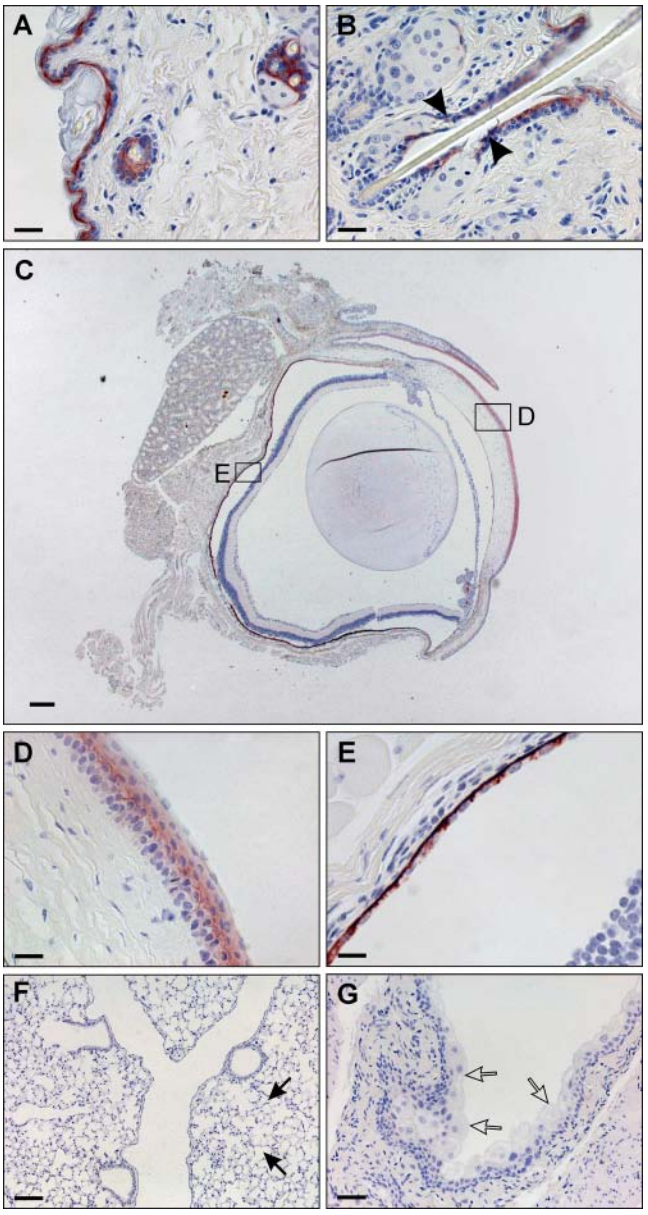

Figure 4. C4.4A expression in the mouse skin, eye, lung, and bladder. Paraffin-embedded tissue sections were incubated with our polyclonal rabbit anti-C4.4A antibody (2.5 µg/ml), stained with immunoperoxidase, and visualized by the NovaRed chromogene. Detection of C4.4A in mouse skin of the mammae is shown in panel A and in the skin-related hair follicle in panel B. A low magnification illustrates the composition of the eye (C), whereas high magnifications of cornea (D) and retina (E) reveal the specific detection of C4.4A in the squamous epithelium and pigmented epithelium, respectively. The lack of C4.4A expression in the epithelia of the lungs (pulmonary epithelium) and bladder (urothelium) is shown in panels F and G, respectively. Arrowheads show the orifice of the sebaceous glands of the hair follicle, black arrows indicate alveolar tissue of the lung, and open arrows point out the quiescent urothelium of the bladder. Scale bars = 400 µm (C), 100 µm (F), 50 µm (G), 25 µm (A, B, D), and 20 µm (E).

E15.5, however, C4.4A was visible in a pronounced membrane-bound appearance (Figure 5F). At E16, the terminal differentiation of the skin is complete, which is characterized by the presence of the outer keratinized epidermal layer, the stratum corneum (Bickenbach et al. 1995; Hanson 1947). The stratum corneum and the underlying stratum granulosum, which are only weakly visible at embryonic day E16.5, are devoid of C4.4A (data not shown). This C4.4A expression pattern, characteristic of the adult epidermis, becomes more pronounced in the later developmental stages.

The vibrissal follicles expressed C4.4A already from day E14.5 (Fig. 5H). The mouse embryo vibrissal follicles appear in an earlier embryogenic stage than the pelage hair follicles, and the formation of the hair canals, which protrude from the epidermis, happens at day E15 (Davidson and Hardy 1952), at the time point where C4.4A expression is induced.

In the upper part of the gastrointestinal tract, C4.4A expression was detectable in the epithelium of the tongue at day E14.5 (data not shown) and weakly in the esophagus at day E15.5 (Fig. 5L). This latter observation coincides with the onset of a columnar-squamous transdifferentiation of the esophageal epithelium (Yu et al. 2005). As opposed to the adult epidermis (Fig. 4A) and esophagus (Fig. 1A,B), which contain a cornified layer devoid of C4.4A expression, the embryonic esophagus lacks this cornification (Parakkal 1967; Raymond et al. 1991), and C4.4A expression is observed throughout the squamous suprabasal layer. Expression was also found in the squamous epithelium of the non-glandular part of the stomach and ano-rectal junction at days E15.5 and E14.5, respectively (data not shown).

Discussion

C4.4A was initially identified as a metastasis-associated protein (Claas et al. 1996), and expression of C4.4A is accordingly observed in various human cancer lesions (Hansen et al. 2008; Hansen et al. 2007; Paret et al. 2007; Smith et al. 2001; Würfel et al. 2001). In NSCLC, its expression levels even carry prognostic information on patient survival (Hansen et al. 2007). Regrettably, however, no solid biochemical function has as yet been assigned to C4.4A. Nevertheless, circumstantial evidence suggests a role for C4.4A in cell-cell or cell-matrix adhesion (Hansen et al. 2008; Paret et al. 2005; Rösel et al. 1998; Smith et al. 2001). To advance our understanding of the putative physiological role of C4.4A in normal and pathological conditions, it is thus imperative to conduct animal studies, where this function has been abrogated by *Lypd3* gene ablation, for example. To enable the functional dissection of any overt phenotypes that may arise in such animal model systems, we have in the present study undertaken a histological

Table 2. Expression of C4.4A in Embryonic Tissues

Tissue	E9.5	E13.5	E14.5	E15.5	E16.5	E17.5	E18.5	Newborn
Nasal cavity	–	+++	+++	+++	+++	+++	+++	ND
Tongue	–	–	+	++	+++	+++	+++	+++
Esophagus	–	–	–	+	+	++	ND	ND
Non-glandular stomach	–	–	–	+	++	+++	+++	+++
Anus	–	–	+	+++	+++	+++	+++	+++
Skin (back)	–	–	+	+++	+++	+++	+++	+++
Skin (paw)	–	+	+	+++	+++	+++	+++	+++
Hair follicle (vibrissae)	–	–	++	+++	+++	+++	+++	+++

Abbreviations: +, weak C4.4A staining intensity or staining of only a few cells; ++, moderate C4.4A staining intensity of cells comprising a single layer of squamous epithelium; +++, strong C4.4A staining of cells constituting a single or a stratified layer of squamous epithelium; –, no C4.4A staining; ND, not determined.

mapping of the C4.4A expression in the normal adult mouse as well as during embryogenesis.

As a general common denominator, we find a pronounced C4.4A expression confined to the cell membrane of all squamous epithelia examined (i.e., the oral cavity, esophagus, non-glandular part of the stomach, cornea, skin, and vagina). In all cases, C4.4A expression is restricted to the suprabasal layer of the epithelium, leaving the basal layer devoid of C4.4A.

This tissue-specific expression profile of C4.4A in squamous epithelia is particularly evident by its abrupt termination upon transition to columnar epithelium at squamo-columnar junctions (Figs. 2 and 3). Such stringent expression patterns call for a tight regulation of the *Lypd3* gene, and this may in part be accomplished by the transcriptional control exerted by C/EBPβ (Fries et al. 2007). In addition, circumstantial evidence also suggests a gene regulatory mechanism through the action of the sex hormone estrogen. An estrogen-induced increase in C4.4A mRNA levels has accordingly been reported in three independent studies (Chisamore et al. 2009; Hardman and Ashcroft 2008; Helvering et al. 2005). Along the same line of arguments, the *Lypd3* gene is also tightly regulated during embryonic development of the mouse, where the first evidence for C4.4A expression emerges in the squamous epithelium of the nasal cavity and outer cell layers of the paws at day E13.5, the vibrissal follicles and back skin at day E14.5, and the esophagus and non-glandular part of the stomach at day E15.5. Interestingly, these results coincide with well-established murine embryonic squamous differentiation programs. In the developing mouse embryo, the expression of the suprabasal differentiation-specific cytokerations 1 and 10 is induced at exactly day E13.5 in the nasal cavity and at day E14.5 in the interfollicular epidermis of the vibrissae (Byrne et al. 1994). In the skin of the paws and back, the cytokeratins 1 and 10 are not expressed until days 14.5 and 15.5, respectively (Bickenbach et al. 1995; Byrne et al. 1994)—that is, one day later than the induction of C4.4A expression. As for the non-glandular part of the mouse stomach, it begins to stratify at embryonic day 13.5, and the formation of a granular and cornified layer is first noted at day E16.5 (Fukamachi et al. 1979). The stratum spinosum thus develops prior to day E16.5, where we also observe the first C4.4A expression.

The esophagus, on the other hand, undergoes a complete columnar-squamous transdifferentiation at days E15.5 to E17.5, with the gradual loss of cytokeratin 8 as a marker for columnar epithelium from day E15.5 and the appearance of cytokeratin 14 as a marker for stratified squamous epithelium at day E17.5 (Yu et al. 2005). Thus, C4.4A expression seems induced at the same time point or prior to the keratins specific for epithelial differentiation. Taken together, these data suggest that C4.4A is a marker of very early stages of squamous differentiation.

The tightly regulated expression of C4.4A in the suprabasal layer of the homeostatic squamous epithelium, which we have uncovered here in the healthy mouse, may actually have a bearing on certain pathophysiological conditions in humans. In particular, the development of preneoplastic lesions in the pulmonary epithelium during progression of NSCLC represents an intriguing case. As shown in Figure 3F, the normal alveolar and bronchial epithelia of non-insulted mouse lungs are completely devoid of C4.4A expression, which aligns excellently with our present proposition of C4.4A as a generalized biomarker for squamous differentiation. In an ongoing study comparing premalignant pulmonary lesions with manifest adenocarcinomas or squamous cell carcinomas in NSCLC patients, we nevertheless observe an interesting progression in C4.4A expression. The morphologically normal-appearing human bronchial epithelia located distantly from any visual lesions are devoid of C4.4A reactivity, thus recapitulating the present findings for murine lungs. The absence of C4.4A expression in the normal human lung has further been confirmed at the mRNA level by RT-PCR and Northern blotting (Würfel et al. 2001). With the onset of metaplasia, as judged

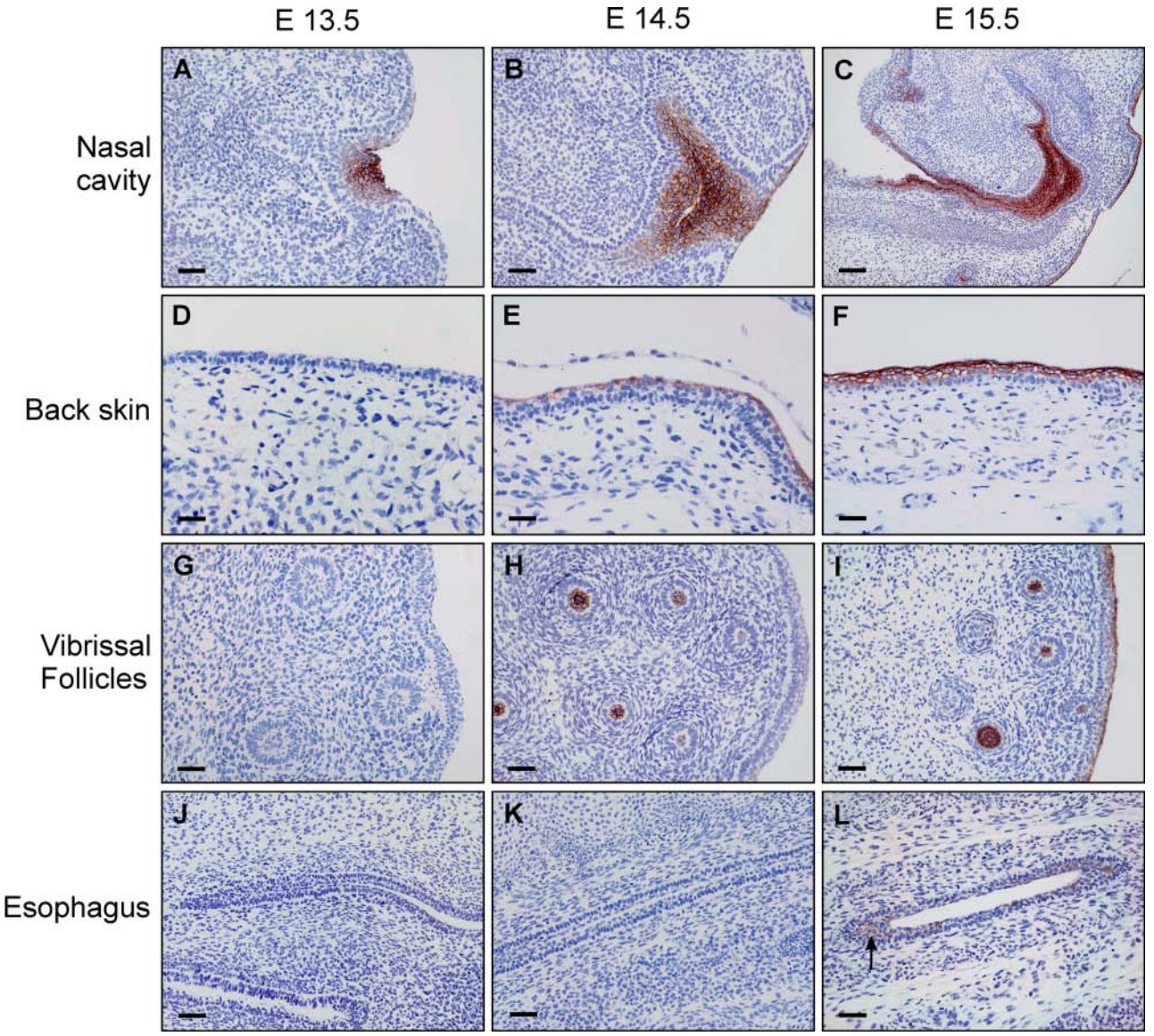

Figure 5. Expression of C4.4A in the nasal cavity, skin, hair follicles, and esophagus of mouse embryos. Serial sections of paraffin-embedded intact embryos were incubated with 2.5 µg/ml polyclonal rabbit anti-C4.4A antibody, and detection of C4.4A was visualized using the NovaRed chromogene. Selected tissues represent embryonic stages 13.5 (A, D, G, J), 14.5 (B, E, H, K), and 15.5 (C, F, I, L) and include nasal cavity (A-C), back skin (D-F), vibrissal hair follicles (G-I), and esophagus (J-L). The arrow in panel L indicates the C4.4A-expressing suprabasal layer of the esophageal squamous epithelium. Scale bars = 100 µm (C), 50 µm (A, B, D, E, F, G, H, I), and 40 µm (J, K, L).

by morphological criteria, we find that a robust and membrane-confined expression of C4.4A is already evident, spanning the entire thickness of the transformed epithelium (Jacobsen et al. 2011). Importantly, the adjacent ciliated epithelium, which appears morphologically normal, often presents a weak but distinct intracellular expression of C4.4A in the basal cells, indicating that C4.4A is a marker of the very early phases of metaplasia paralleling the situation observed in embryonic tissue of the mouse. With a view to the induction of C4.4A expression already at this non-malignant histopathological stage, it is noteworthy that the frequency and expression levels of C4.4A in the resected tumor tissues from NSCLC patients do not provide prognostic information on patient survival if they are diagnosed with a squamous cell carcinoma (Hansen et al. 2007). Quite the opposite pertains to NSCLC patients with diagnosed adenocarcinomas, where a high C4.4A expression level is a powerful prognostic biomarker for poor survival (Hansen

et al. 2007). This distinction is really intriguing because our present expression profiling of C4.4A in the normal mouse never detected any C4.4A expression in the cell types associated with the normal columnar epithelia from which the adenocarcinomas usually originate. Although the pathogenesis of pulmonary NSCLC adenocarcinomas is less well established, atypical adenomatous hyperplasia (AAH) is often considered a precursor lesion of adenocarcinoma (Wistuba and Gazdar 2006). Interestingly, we find that a certain fraction of AAH lesions contains numerous type II pneumocytes that do in fact express C4.4A intracellularly (Jacobsen et al. 2011). It is thus possible that these cells are responsible for the atypical expression of C4.4A observed later on in the malignant progression to the manifest, invasive adenocarcinomas (Hansen et al. 2007). The perturbation(s) in the molecular pathway(s) responsible for this aberrant expression of C4.4A, however, remains to be clarified.

Another pathological condition, in which an atypical expression of C4.4A unexpectedly emerges in the transformed "non-squamous epithelium," is represented by the transitional cell carcinoma of the human bladder. In the present study, we find C4.4A expression to be undetectable by immunohistochemistry in the quiescent urothelium of both mouse and rat bladder. Nonetheless, upon progression of the urothelium to transitional cell carcinoma, C4.4A mRNA levels are upregulated in both the primary tumor mass as well as the corresponding metastatic foci in distant lymph nodes (Smith et al. 2001). Interestingly, the same study also proposed that the *LYPD3* gene may be a part of the wound response program in normal human urothelial cells, as these upregulate C4.4A when exposed to extracellular matrix proteins (Smith et al. 2001).

To enable a meticulous interrogation of the putative functional role of C4.4A in vivo for maintenance of normal squamous epithelial integrity and for testing its impact on the pathogenesis of carcinomas in particular, it is mandatory to establish relevant in vivo mouse models. Currently, we aim at generating a transgenic mouse strain deficient for C4.4A by the gene ablation of *Lypd3*. As judged from our present expression profiling of C4.4A during mouse embryogenesis, we do not expect to encounter any increased lethality in such transgenic mice before day E13.5, when the earliest C4.4A expression emerges in the embryonic nasal cavity and skin. If such C4.4A-deficient mice are indeed viable, it will be interesting to test the integrity of their epithelial barrier function as well as the kinetics of keratinocyte migration during closure of incisional skin wounds. With a view to epithelial integrity, a puzzling but circumstantial observation is the recent discovery that the assembly and intact barrier function of septate junctions in *Drosophila* are critically dependent on a number of small glycolipid-anchored proteins (*crok*, *cold*, *crim*, and *boudin*), which are composed of a single LU domain and thus are structural homologs of C4.4A (Hijazi et al. 2009; Nilton et al. 2010). The connection to wound healing is more direct, as a previous study demonstrated a clear upregulation of C4.4A expression in the migrating murine keratinocytes during healing of incisional skin wounds (Hansen et al. 2004). Furthermore, a microarray study comparing skin wound healing in young versus old healthy subjects has reported that the keratinocytes of elderly humans have a decreased C4.4A expression (Hardman and Ashcroft 2008) as well as an attenuated migratory phenotype (Holt et al. 1992).

Finally, it will be interesting to scrutinize the impact of C4.4A on the pathogenesis of NSCLC with particular emphasis on the histological subtype of adenocarcinomas. The clinical relevance of this is highlighted both by the C4.4A expression in the corresponding premalignant lesions (Jacobsen et al. 2011) and by the prognostic value of C4.4A expression levels for survival of this group of cancer patients (Hansen et al. 2007). The applicability of a C4.4A-deficient mouse strain for such studies is straightforward as several mouse models exist for induction of NSCLC of the adenocarcinoma subtype both by genetic aberrations (DuPage et al. 2009; Meuwissen and Berns 2005) and by chemical insult (Meuwissen and Berns 2005).

Acknowledgments

We acknowledge Dr. Ole Didrik Lærum for his constructive comments on the manuscript as well as the excellent technical assistance of John Post on creating the photographic artwork.

Declaration of Conflicting Interests

The author(s) declared no potential conflicts of interest with respect to the authorship and/or publication of this article.

Funding

The author(s) disclosed receipt of the following financial support for the research and/or authorship of this article: This work was supported financially by the Copenhagen University Hospital (Rigshospitalet), Denmark; The Danish National Research Foundation (Danish-Chinese Centre for Proteases and Cancer); Dansk Kræftforsknings Fond; Axel Muusfeldts Fond; Fabrikant Einar Willumsens Mindelegat; C. C. Klestrup og Hustru Henriette Klestrups Mindelegat; Civilingeniør H. C. Bechgaard og Hustru Ella Mary Bechgaards Fond; and Max Fodgaard Fonden.

References

Bickenbach JR, Greer JM, Bundman DS, Rothnagel JA, Roop DR. 1995. Loricrin expression is coordinated with other epidermal proteins and the appearance of lipid lamellar granules in development. J Invest Dermatol. 104:405-410.

Bos PD, Nguyen DX, Massague J. 2010. Modeling metastasis in the mouse. Curr Opin Pharmacol. 10:1-7.

Byrne C, Tainsky M, Fuchs E. 1994. Programming gene expression in developing epidermis. Development. 120:2369-2383.

Chisamore MJ, Wilkinson HA, Flores O, Chen JD. 2009. Estrogen-related receptor-alpha antagonist inhibits both estrogen receptor-positive and estrogen receptor-negative breast tumor growth in mouse xenografts. Mol Cancer Ther. 8:672-681.

Claas C, Herrmann K, Matzku S, Möller P, Zöller M. 1996. Developmentally regulated expression of metastasis-associated antigens in the rat. Cell Growth Differ. 7:663-678.

Connolly BM, Choi EY, Gårdsvoll H, Bey AL, Currie BM, Chavakis T, Liu S, Molinolo A, Ploug M, Leppla SH, et al. 2010. Selective abrogation of the uPA-uPAR interaction in vivo reveals a novel role in suppression of fibrin-associated inflammation. Blood. 116:1593-1603.

Davidson P, Hardy MH. 1952. The development of mouse vibrissae in vivo and in vitro. J Anat. 86:342-356.

DuPage M, Dooley AL, Jacks T. 2009. Conditional mouse lung cancer models using adenoviral or lentiviral delivery of Cre recombinase. Nat Protoc. 4:1064-1072.

Fries F, Nazarenko I, Hess J, Claas A, Angel P, Zöller M. 2007. CEBPbeta, JunD and c-Jun contribute to the transcriptional activation of the metastasis-associated C4.4A gene. Int J Cancer. 120:2135-2147.

Fukamachi H, Mizuno T, Takayama S. 1979. Epithelial-mesenchymal interactions in differentiation of stomach epithelium in fetal mice. Anat Embryol (Berl). 157:151-160.

Gårdsvoll H, Hansen LV, Jørgensen TJ, Ploug M. 2007. A new tagging system for production of recombinant proteins in Drosophila S2 cells using the third domain of the urokinase receptor. Protein Expr Purif. 52:384-394.

Hansen LV, Gårdsvoll H, Nielsen BS, Lund LR, Danø K, Jensen ON, Ploug M. 2004. Structural analysis and tissue localization of human C4.4A: a protein homologue of the urokinase receptor. Biochem J. 380:845-857.

Hansen LV, Lærum OD, Illemann M, Nielsen BS, Ploug M. 2008. Altered expression of the urokinase receptor homologue, C4.4A, in invasive areas of human esophageal squamous cell carcinoma. Int J Cancer. 122:734-741.

Hansen LV, Skov BG, Ploug M, Pappot H. 2007. Tumour cell expression of C4.4A, a structural homologue of the urokinase receptor, correlates with poor prognosis in non–small cell lung cancer. Lung Cancer. 58:260-266.

Hanson J. 1947. The histogenesis of the epidermis in the rat and mouse. J Anat. 81:174-197.

Hardman MJ, Ashcroft GS. 2008. Estrogen, not intrinsic aging, is the major regulator of delayed human wound healing in the elderly. Genome Biol. 9:R80.

Helvering LM, Adrian MD, Geiser AG, Estrem ST, Wei T, Huang S, Chen P, Dow ER, Calley JN, Dodge JA, et al. 2005. Differential effects of estrogen and raloxifene on messenger RNA and matrix metalloproteinase 2 activity in the rat uterus. Biol Reprod. 72:830-841.

Hijazi A, Masson W, Auge B, Waltzer L, Haenlin M, Roch F. 2009. Boudin is required for septate junction organisation in Drosophila and codes for a diffusible protein of the Ly6 superfamily. Development. 136:2199-2209.

Holt DR, Kirk SJ, Regan MC, Hurson M, Lindblad WJ, Barbul A. 1992. Effect of age on wound healing in healthy human beings. Surgery. 112:293-297; discussion 297-298.

Høyer-Hansen G, Lund IK. 2007. Urokinase receptor variants in tissue and body fluids. Adv Clin Chem. 44:65-102.

Huai Q, Mazar AP, Kuo A, Parry GC, Shaw DE, Callahan J, Li Y, Yuan C, Bian C, Chen L, et al. 2006. Structure of human urokinase plasminogen activator in complex with its receptor. Science. 311:656-659.

Ito M. 1986. The innermost cell layer of the outer root sheath in anagen hair follicle: light and electron microscopic study. Arch Dermatol Res. 279:112-119.

Jacobsen B, Ploug M. 2008. The urokinase receptor and its structural homologue C4.4A in human cancer: expression, prognosis and pharmacological inhibition. Curr Med Chem. 15:2559-2573.

Jacobsen B, Santoni-Rugiu E, Illemann M, Lærum OD, Ploug M. 2011. Expression of C4.4A in precursor lesions of non-small cell lung cancer. Int J Cancer. Manuscript submitted.

Kjaergaard M, Hansen LV, Jacobsen B, Gårdsvoll H, Ploug M. 2008. Structure and ligand interactions of the urokinase receptor (uPAR). Front Biosci. 13:5441-5461.

Lin L, Gårdsvoll H, Huai Q, Huang M, Ploug M. 2010. Structure-based engineering of species selectivity in the interaction between urokinase and its receptor: implication for preclinical cancer therapy. J Biol Chem. 285:10982-10992.

Llinas P, Le Du MH, Gårdsvoll H, Danø K, Ploug M, Gilquin B, Stura EA, Menez A. 2005. Crystal structure of the human urokinase plasminogen activator receptor bound to an antagonist peptide. EMBO J 24:1655-1663.

Meuwissen R, Berns A. 2005. Mouse models for human lung cancer. Genes Dev. 19:643-664.

Nilton A, Oshima K, Zare F, Byri S, Nannmark U, Nyberg KG, Fehon RG, Uv AE. 2010. Crooked, coiled and crimpled are three Ly6-like proteins required for proper localization of septate junction components. Development. 137:2427-2437.

Parakkal PF. 1967. An electron microscopic study of esophageal epithelium in the newborn and adult mouse. Am J Anat. 121:175-195.

Paret C, Bourouba M, Beer A, Miyazaki K, Schnolzer M, Fiedler S, Zöller M. 2005. Ly6 family member C4.4A binds laminins 1 and 5, associates with galectin-3 and supports cell migration. Int J Cancer. 115:724-733.

Paret C, Hildebrand D, Weitz J, Kopp-Schneider A, Kuhn A, Beer A, Hautmann R, Zöller M. 2007. C4.4A as a candidate marker in the diagnosis of colorectal cancer. Br J Cancer. 97:1146-1156.

Ploug M. 2003. Structure-function relationships in the interaction between the urokinase-type plasminogen activator and its receptor. Curr Pharm Des. 9:1499-1528.

Raymond C, Anne V, Millane G. 1991. Development of esophageal epithelium in the fetal and neonatal mouse. Anat Rec. 230:225-234.

Rösel M, Claas C, Seiter S, Herlevsen M, Zöller M. 1998. Cloning and functional characterization of a new phosphatidyl-inositol anchored molecule of a metastasizing rat pancreatic tumor. Oncogene. 17:1989-2002.

Seiter S, Stassar M, Rappl G, Reinhold U, Tilgen W, Zöller M. 2001. Upregulation of C4.4A expression during progression of melanoma. J Invest Dermatol. 116:344-347.

Shezen E, Okon E, Ben-Hur H, Abramsky O. 1995. Cytokeratin expression in human thymus: immunohistochemical mapping. Cell Tissue Res. 279:221-231.

Smith BA, Kennedy WJ, Harnden P, Selby PJ, Trejdosiewicz LK, Southgate J. 2001. Identification of genes involved in human urothelial cell-matrix interactions: implications for the progression pathways of malignant urothelium. Cancer Res. 61:1678-1685.

Ullah MF, Aatif M. 2009. The footprints of cancer development: cancer biomarkers. Cancer Treat Rev. 35:193-200.

Westwood FR. 2008. The female rat reproductive cycle: a practical histological guide to staging. Toxicol Pathol. 36:375-384.

Wistuba II, Gazdar AF. 2006. Lung cancer preneoplasia. Annu Rev Pathol. 1:331-348.

Würfel J, Seiter S, Stassar M, Claas A, Klas R, Rösel M, Marhaba R, Savelyeva L, Schwab M, Matzku S, et al. 2001. Cloning of the human homologue of the metastasis-associated rat C4.4A. Gene. 262:35-41.

Yu WY, Slack JM, Tosh D. 2005. Conversion of columnar to stratified squamous epithelium in the developing mouse oesophagus. Dev Biol. 284:157-170.